

MSEC2017-2739

RAPID INTENSE PULSE LIGHT SINTERING OF COPPER SULPHIDE NANOPARTICLE FILMS

Shalu Bansal

Department of Mechanical Engineering,
Oregon State University,
Corvallis, Oregon, USA

Zhongwei Gao

School of Chemical, Biological and Environmental
Engineering,
Oregon State University,
Corvallis, Oregon, USA

Chih-hung Chang

School of Chemical, Biological and Environmental
Engineering,
Oregon State University,
Corvallis, Oregon, USA

Rajiv Malhotra

Department of Mechanical Engineering,
Oregon State University,
Corvallis, Oregon, USA

ABSTRACT

Copper sulphide (Cu_xS , $x=1$ to 2) is a metal chalcogenide semiconductor that exhibits useful optical and electrical properties due to the presence of copper vacancies. This makes Cu_xS thin films useful for a number of applications including infrared absorbing coatings, solar cells, thin-film electronics, and as a precursor for CZTS (Copper Zinc Tin Sulphide) thin films. Post-deposition sintering of Cu_xS nanoparticle films is a key process that affects the film properties and hence determines its operational characteristics in the above applications. Intense pulse light (IPL) sintering uses visible broad-spectrum xenon light to rapidly sinter nanoparticle films over large-areas, and is compatible with methods such as roll-to-roll deposition for large-area deposition of colloidal nanoparticle films and patterns. This paper experimentally examines the effect of IPL parameters on sintering of Cu_xS thin films. As-deposited and sintered films are compared in terms of their crystal structure, as well as optical and electrical properties, as a function of the IPL parameters.

INTRODUCTION

Copper sulphide (Cu_xS where $x = 1-2$) is a non-toxic and earth-abundant transition-metal chalcogenide with an optical band gap of 1.2-2.5 eV [1]. Cu_xS also shows p-type semiconducting behavior due to presence of copper vacancies. Copper sulphide thin films are used in a variety of application including Lithium ion batteries [2], transparent conductive layers

in electroluminescent devices [3], thin film transistors [4], p-type absorber in solar cells [5,6] and infrared absorbing coatings [7] on windows. These applications generally require highly crystalline films with desired electrical and optical properties.

Cu_xS thin films have been deposited using various solution-based approaches like SILAR (Successive Ionic Layer Adsorption and Reaction) [8], CBD (Chemical Bath Deposition) [9] and vacuum based methods like ALD (Atomic Layer Deposition) [10,11] and thermal evaporation [4]. More recently the potential for depositing such films by inkjet printing or roll-to-roll printing of solution-based nanoparticles has emerged as well. In order to obtain crystalline films with desired properties, sintering of the deposited film is a key post-deposition step. Conventional thermal annealing in a furnace typically needs up to an hour [12,13]. On the other hand Rapid Thermal Annealing or RTA [14] reduces the annealing time to around 5 minutes by employing heating rate of around 25 °C/s to a temperature of 200-500 °C in a furnace. However, even this higher throughput of RTA is incompatible with high speed solution-based deposition processes like roll-to-roll deposition and inkjet printing.

Recently Intense Pulsed Light sintering (IPL) has emerged as a process for rapid ambient condition sintering of nanoparticles. IPL uses pulsed broad-spectrum (300-700 nm), visible light from a Xenon Lamp over a relatively large area (12" x 0.75") to heat the nanoparticles and cause sintering (Fig. 1). This creates the possibility that IPL can be used to sinter

nanoparticles over a large area under ambient conditions, and can therefore be compatible with roll-to-roll deposition speeds if the IPL sintering speed is high enough.

IPL has been demonstrated for metallic nanoparticles like Ag [15,16], Cu [17,18] and semiconducting nanoparticles like CdS [19], CdTe [20], CIGS or CuInGaS [21], and CZTS or CuZnSnS [22]. However, IPL of Cu_xS thin films is unexplored till date.

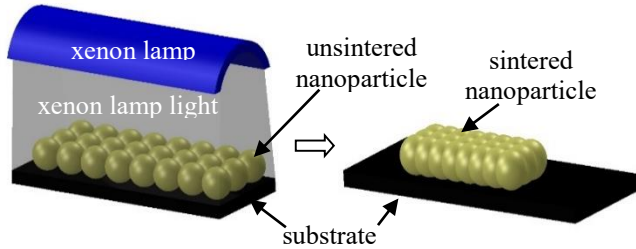


Figure 1: Schematic of IPL

This work examines the IPL of Cu_xS thin films. Specifically, the electrical properties, crystalline phase and optical properties of the thin films are examined as a function of IPL parameters. The optical energy density, pulse number, pulse duration and pulse off time in IPL are varied to determine their effects on properties of the Cu_xS thin film properties. The effect of the observed properties and the throughput of IPL on the processing of Cu_xS thin films is discussed.

EXPERIMENTAL METHODS

Copper sulphide thin films were deposited on glass substrates of size 2.54 cm by 1.9 cm through Chemical Bath deposition as in [9], as shown in Fig. 2a. A typical chemical bath was composed of 7.49g of copper (II) sulfate ($\text{CuSO}_4 \cdot 5\text{H}_2\text{O}$ Alfa Aesar), 2.46g of sodium acetate (CH_3COONa , Macron), 33.78g of triethanoamine ($\text{C}_6\text{H}_5\text{NO}_3$, Sigma), 15.2ml ammonium hydroxide (28%.0-30.0% NH_3 , Macron) dissolved in 100ml of DI water. Additional 20ml of 1.5M thiourea ($\text{CH}_4\text{N}_2\text{S}$, Sigma-Aldrich) solution was added to the bath, followed by adding extra DI water until the total volume of the solution reached 300ml. The chemical bath was stirred and placed into a water bath at a temperature of 45°C on hot plate. The glass substrates were immersed vertically into the chemical bath solution for about 50 min and the film was grown on the substrates. After the deposition, the substrates were rinsed by DI water and dried by

nitrogen gas. The thickness of these films as measured via Scanning Electron Microscopy was 100 ± 10 nm.

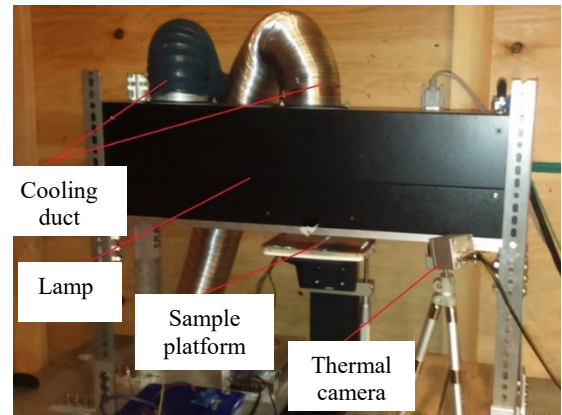
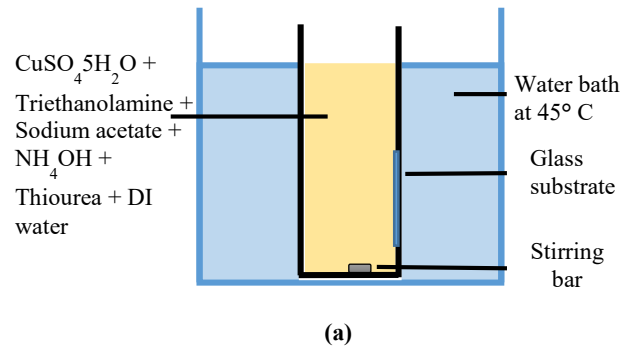


Figure 2: (a) Schematic of Chemical Bath deposition method (b) Experimental setup of IPL system, used in this work

The experimental setup for IPL (fig 2b) consisted of the IPL lamp and a sample platform. The xenon lamp was a Sinteron 3000 system (from Xenon Corporation) with an optical footprint of 12" by 0.75" at a distance of 1" from the lamp. For this xenon lamp, the operating voltage V and pulse on-time t_{on} determines the fluence per pulse E_p according to $E_p = t_{on} \times (V/3120)^{2.4}$. Further note that at any given combination of on-time and voltage there is a minimum off-time that is needed for charging the capacitor network powering the xenon lamp. This minimum off-time was provided by the lamp manufacturer. The Cu_xS deposited glass samples were placed on the sample stage at a distance of 1.5 inch from the lamp.

In the first set of experiments, on-time was varied while the number of pulses was fixed at 5 and the fluence at the substrate was fixed at four different levels E1-E4 (Table 1). Across different on-times, the fluence was kept the same by changing the voltage as per the earlier mentioned relationship. Note that while changing the on-time, the duty cycle of pulsing was kept constant here and the fluence was kept constant by changing the voltage at each on-time. This set of experiments allowed us to examine the effect of increasing on-time while retaining the

same fluence, as well as increasing the fluence by increasing the on-time, on the properties and microstructure of the Cu_xS films.

TABLE 1: VARYING ENERGY DENSITY AT DIFFERENT VOLTAGES FOR 5 PULSES

Optical fluence (J/cm^2)	Voltage (V)		
	V3 = 3000	V2 = 2850	V1 = 2700
	On-time 3/ off-time (ms)	On-time 2 / off-time (ms)	On-time 1/ off-time (ms)
E1= 5	0.715/471	0.810/507	0.925/549
E2= 7.5	1.075/709	1.215/761	1.385/822
E3= 10	1.435/947	1.625/1018	1.845/1096
E4= 15	2.150/1419	2.430/1523	2.770/1645

In the second set of experiments (Table 2), the off-time was increased to two times and three times the minimum off time at a fixed voltage of 3000 V for 5 pulses. The on-times were set such that the fluence per pulse at the substrate was the same as E1-E4 in Table 1. This allowed us to examine the effect of a longer cooling cycle between the pulses on the properties of the Cu_xS film.

TABLE 2: VARYING OFF-TIME AT 3000 V FOR EACH ENERGY DENSITY FOR 5 PULSES

Optical fluence (J/cm^2)	On-time (ms)	Off-time (ms)
E1= 5.0	0.715	471, 471*2, 471*3
E2= 7.5	1.075	709, 709*2, 709*3
E3= 10.0	1.435	947, 947*2, 947*3
E4= 15.0	2.150	1419, 1419*2, 1419*3

The last set of experiments varied the number of pulses from 2, 5 and 10 pulses for each optical fluence E1-E4 at a fixed voltage of 3000 V (Table 3). Note that increasing the number of pulses at the same optical fluence, on-time and off-time essentially increases the total amount of energy deposited on the thin film.

TABLE 3: VARYING NUMBER OF PULSES AT 3000 V FOR EACH ENERGY DENSITY

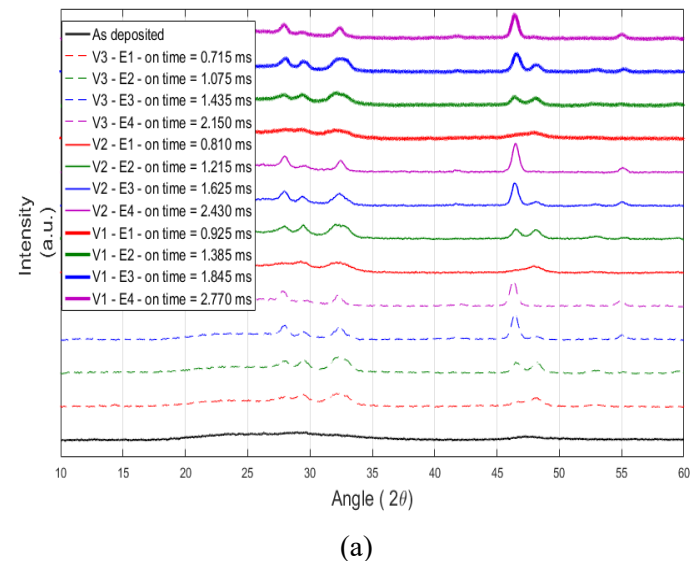
Optical fluence (J/cm^2)	On-time (ms)	Off-time (ms)	Number of pulses
E1= 5.0	0.715	471	2, 5, 10 pulses
E2= 7.5	1.075	709	
E3= 10.0	1.435	947	
E4= 15.0	2.150	1419	

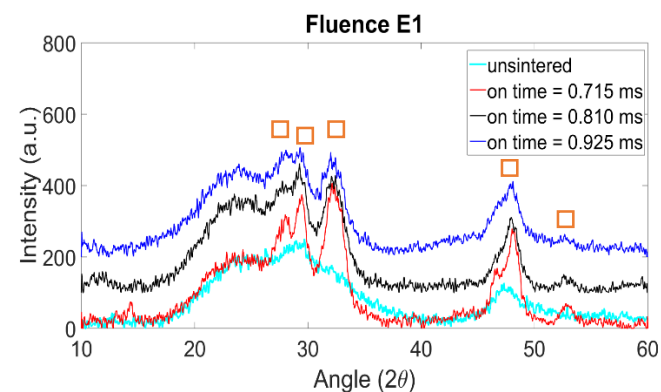
The phase and crystallinity of the films were measured using the GIXRD scan from $2\theta = 10^\circ$ to 60° with a fixed grazing angle of 0.35° on a Rigaku Ultima-IV X-ray diffractometer. The optical properties were measured using transmittance and reflectance (using the integrated sphere method) in a JASCO V670 UV-visible spectrophotometer within the spectral range of 300 nm to 2000 nm and band gap was calculated from the transmittance. Sheet resistance was measured using Signatone four-point probe with probe spacing of 1.588 mm and probe radius of 0.508 mm at five spots on the film.

RESULTS

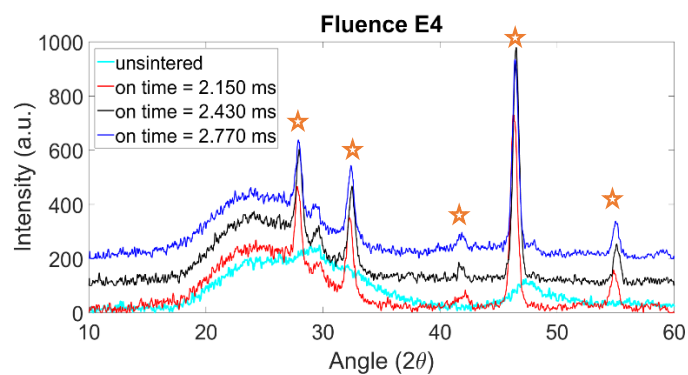
X ray diffraction (XRD) was performed for all the sintered and unsintered samples, and the intensity vs. 2θ curves are shown in Fig. 3. The as-deposited film could not produce any sharp peaks, indicating that the as-deposited film was highly amorphous. Figure 3 shows that in general IPL results in greater crystallinity of the film, indicating the occurrence of sintering. Overall, increasing the fluence results in the initial formation of covellite (CuS)-digenite ($\text{Cu}_{1.8}\text{S}$) phase eventually resulting in the formation of a pure digenite ($\text{Cu}_{1.8}\text{S}$) phase only (Fig. 3a). This is because of an increase in temperature with increasing fluence which results in a phase transformation from a covellite-digenite phase to a pure digenite phase.

Increasing the on-time at a constant fluence per pulse effectively increases the temperature rise per pulse. At lower fluence (E1, Fig. 3b) a predominantly covellite phase is retained (at $2\theta \approx 48^\circ$). At higher fluence values (Figs. 3c-d) an increase in the on-time results in relative increase in digenite content as compared to covellite content as indicated by the relative reduction in covellite peak intensity as compared to the digenite peak intensity at $2\theta \approx 46.7^\circ$. This makes sense because the temperature is expected to be higher at higher on-time. At the highest energy intensity used here (Fig. 3e) there is almost pure digenite phase in the material at any on-time used and the above effect of on-time is not seen.

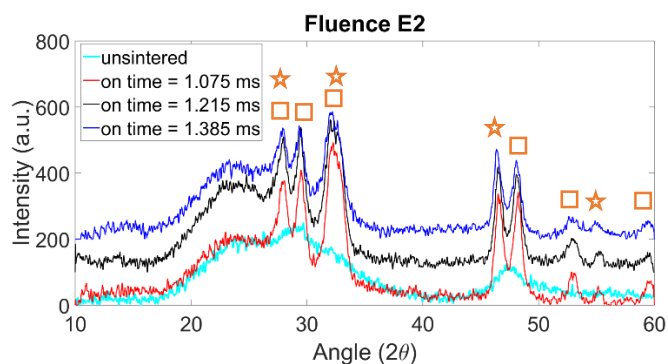




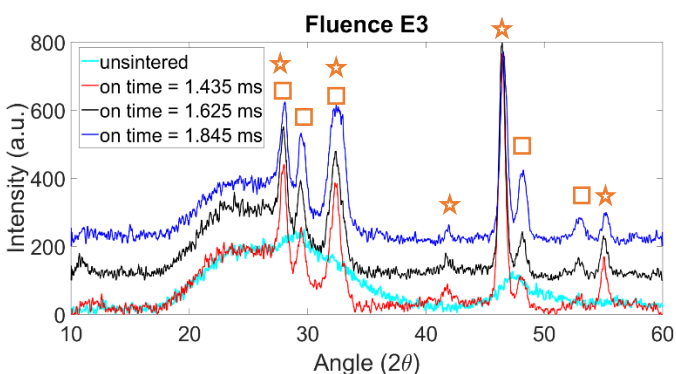
(b)



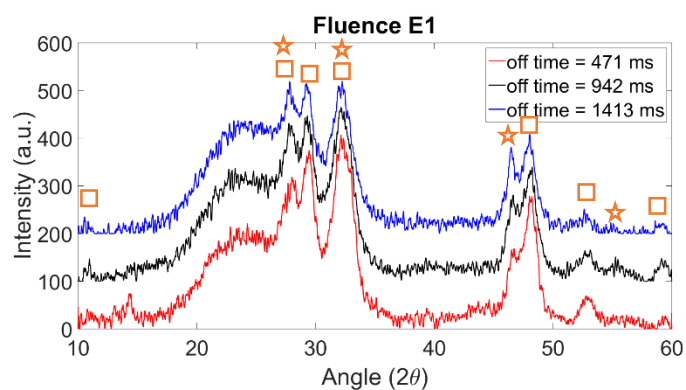
(e)



(c)



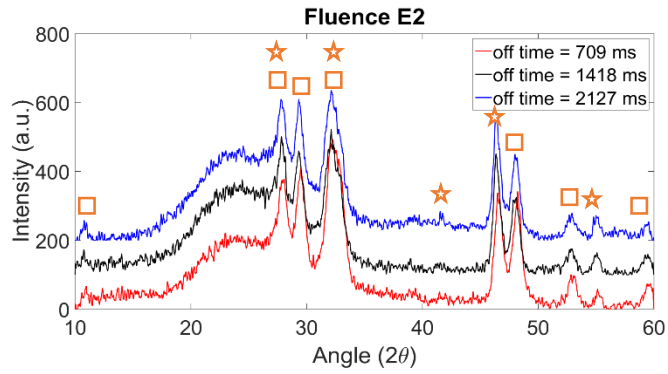
(d)



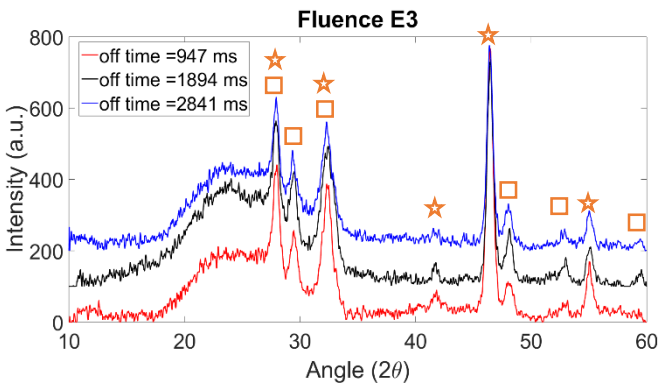
(a)

Figure 3: Effect of on-time in IPL on crystal structure of the Cu_xS thin film. Individual lines within a plot have been translated by 100 a.u. for ease of viewing. Symbol \square is for covellite and \star is for digenite peaks.

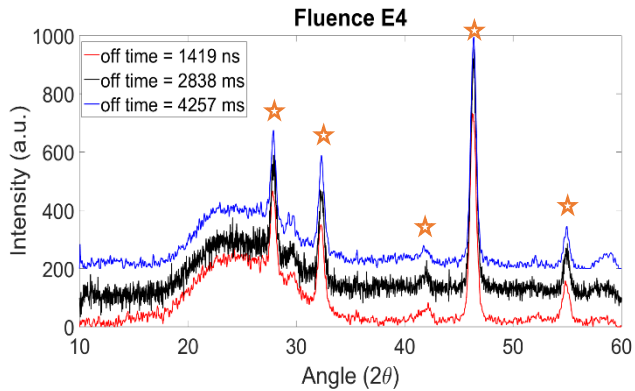
Interestingly, increasing the off-time at a constant fluence for 5 number of pulses seems to increase the relative content of digenite vs covellite in the thin film (Fig.4). Of course, again for fluence E4 this effect is not seen since the fluence causes enough temperature rise for a near complete transformation to the digenite phase. In general an increase in off-time results in a smaller increase in temperature within consecutive pulses. So at a smaller off-time the temperature rise with the same number of pulses in IPL should be greater, thus resulting in greater digenite phase than covellite phase. However, the contrary effect is observed here.



(b)

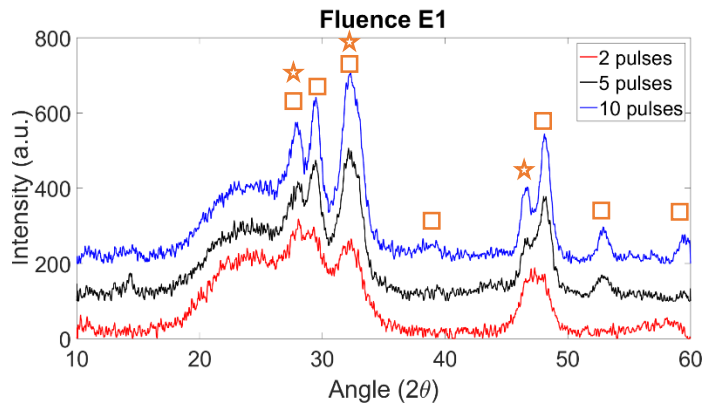


(c)

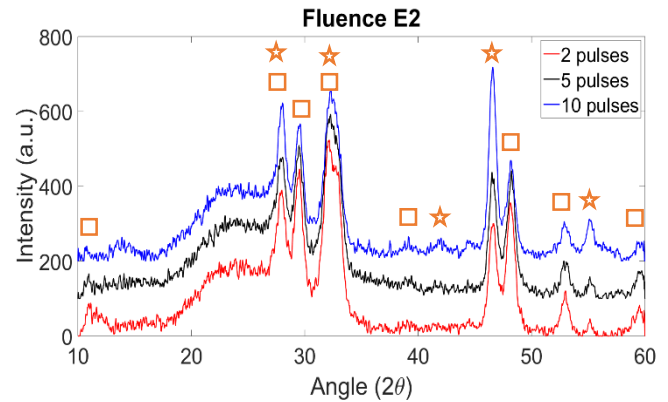


(d)

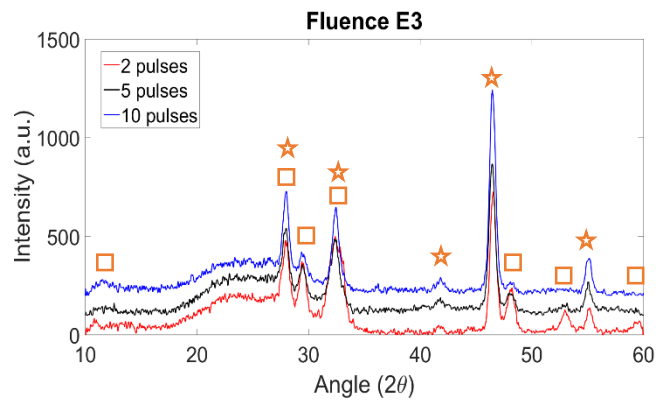
The increase in the number of pulses, essentially resulting in greater total energy deposition, results in an increase in the covellite to digenite transformation, as seen in Fig. 5.



(a)



(b)



(c)

Figure 4: Effect of off-time in IPL on crystal structure of the Cu_xS thin film. Individual lines within a plot have been translated by 100 a.u. for ease of viewing. Symbol \square is for covellite and \star is for digenite peaks.

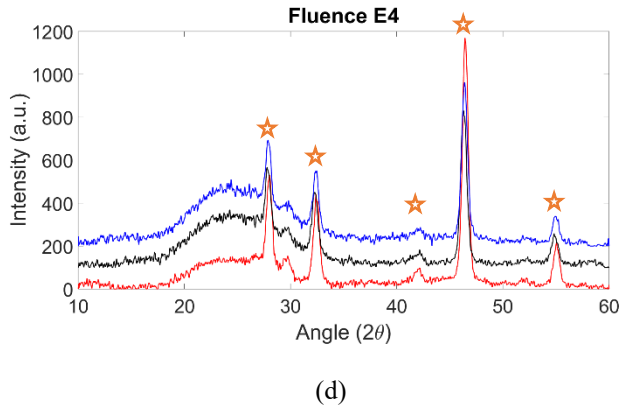
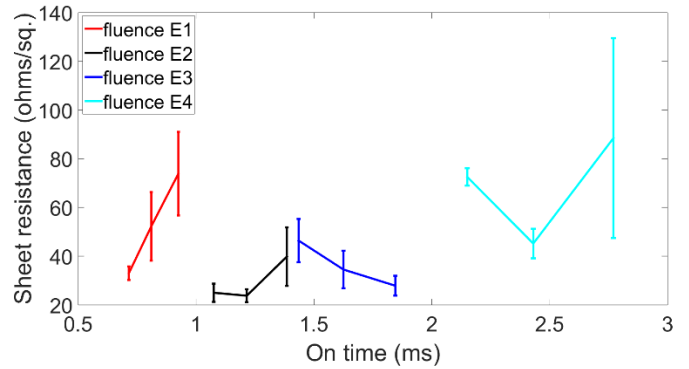
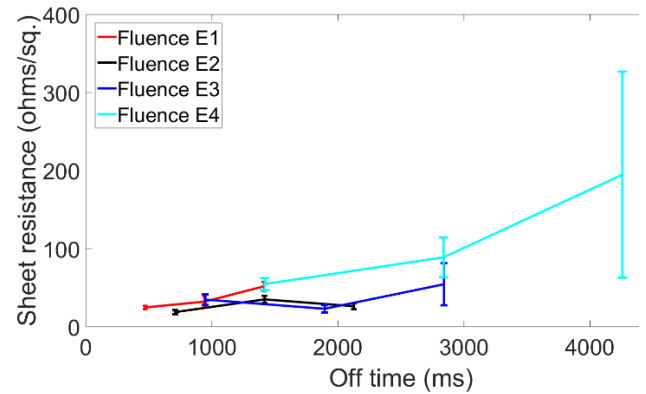


Figure 5: Effect of number of pulses in IPL on crystal structure of the Cu_xS thin film. Individual lines within a plot have been translated by 100 a.u. for ease of viewing. Symbol \square is for covellite and \star is for digenite peaks.

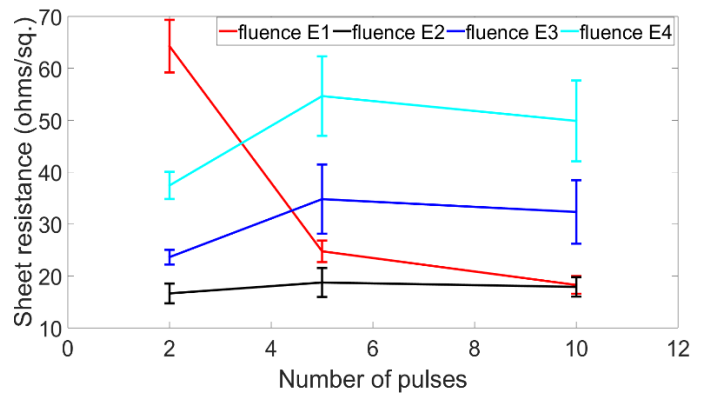
The mean sheet resistance of the as-deposited samples was measured to be 3.66 k Ω /sq. In general, increasing the energy density results in a reduction in sheet resistance due to sintering of the nanoparticles followed by an increase in resistance at a high energy density due to the formation of a nearly pure digenite phase as compared to a mixed covellite-digenite phase. Increasing the on time (Fig. 6a) for a given energy density results in a general increase in sheet resistance (Fig. 3b-3e) as the Cu_xS is transformed from a mixed covellite-digenite to a more digenite phase and the digenite phase has a higher resistivity than the covellite phase. Since increasing the off-time increases the relative amount of digenite to covellite phases in the thin film, the increase in off-time also increases the sheet resistance of the film (Fig. 6b). At fluence E1, going from 2 to 5 pulses significantly reduces the sheet resistance (Fig. 6c) because of grain growth due to sintering and retention of a primarily covellite phase (Fig. 5a). Beyond 5 pulses the covellite to digenite transformation starts to occur (Fig. 5a) and the reduction in resistance is lesser (Fig. 6c). At higher fluences the sheet resistance initially increases due to the transformation to a primarily digenite phase (Fig. 5b-5d), and then undergoes a relatively smaller reduction (Fig. 6c) which is likely due to grain growth rather than phase transformation. Literature reports a sheet resistance value of 6 Ω /sq for covellite and 15 Ω /sq for digenite phase obtained after thermal annealing for one hour in nitrogen atmosphere of 500 nm thick as-deposited films (180 Ω /sq) at a temperature of 200 $^\circ\text{C}$ and 300 $^\circ\text{C}$ [13]. Note that the time taken for this kind of conventional thermal annealing is significantly greater than the few seconds taken in these IPL experiments and the potential of IPL to do the same over large areas (at least 12 x 0.75 sq. inches).



(a)



(b)

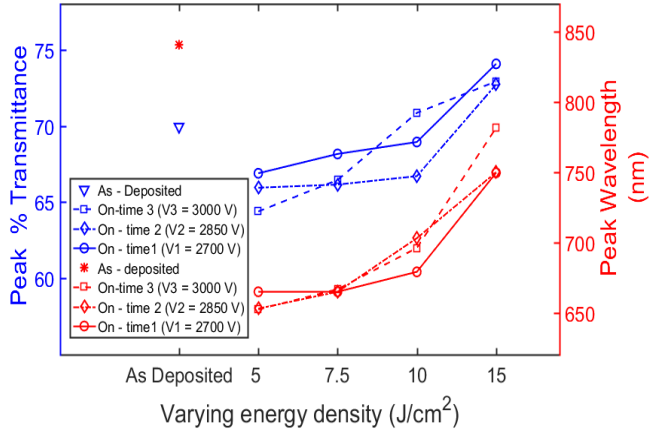


(c)

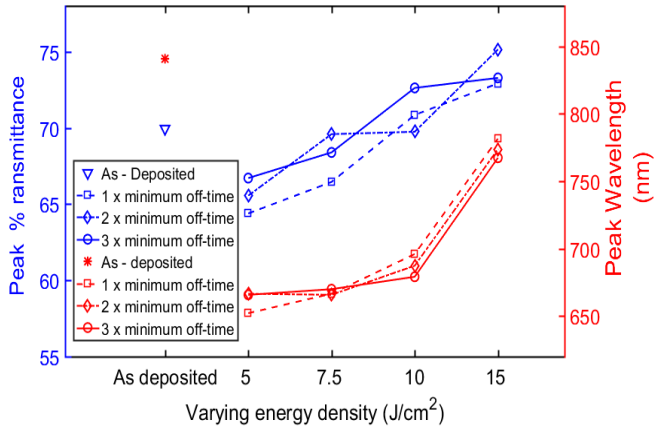
Figure 6: Effect of (a) on-time (b) off-time (c) number of pulses in IPL on sheet resistance of the Cu_xS thin film.

Transmittance for the unsintered samples was 70% in the Near Infrared (NIR) region. Figure 7 shows the peak transmittance and the wavelength corresponding to this peak transmittance for

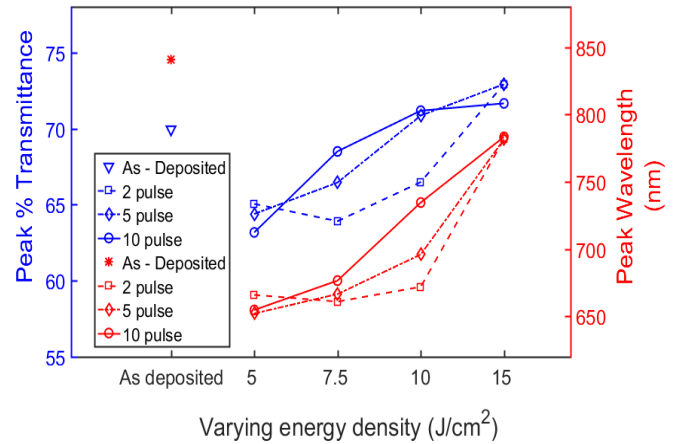
all the sintered samples. Initially, IPL results in a reduction in peak intensity of transmittance and a blue-shift in the corresponding wavelength. As the fluence in IPL increases, the peak transmittance increases beyond that of the unsintered film. Further there is an additional red-shift that shift the wavelength at peak intensity back into the near infrared region, but never as far as that of the unsintered film.



(a)



(b)



(c)

Figure 7: Effect of a) on time for 5 pulses b) off time for 5 pulse c) pulse count in IPL on the peak transmittance intensity and the corresponding wavelength

The band gap (E_g) of the films was estimated using the Tauc Plot. A plot of $(\alpha h\nu)^2$ against the photon energy $h\nu$ shows a linear regime and hence exhibits direct transition band gap. The linear regime is extrapolated to the abscissa and the intercept gives the energy of the optical band gap (where α is the absorption coefficient, h is the Planck's constant and ν is the frequency). The absorption coefficient α was calculated based on $\alpha = \frac{1}{d} \ln \frac{100}{T}$, where d is the thickness of the film at 100 nm, T is the transmittance spectral data. As shown in Fig. 8, we observed a slight increase in the band gap after IPL, ranging between 2.45 eV to 2.55 eV for different phase. The shift in the band gap after annealing can be associated to change in the stoichiometry, i.e., a decreasing Sulphur content. The band gap for the as-deposited films was 2.4 eV which is similar to values of 2.2-2.4 eV reported in literature for Cu_xS films [23–25].

Fluence	Phase	Band gap (eV)
0	Unsintered film	2.40
E1	More Covellite	2.45
E2	Mixed Covellite+ Digenite	2.52
E3	More Digenite	2.55
E4	Digenite only	2.50

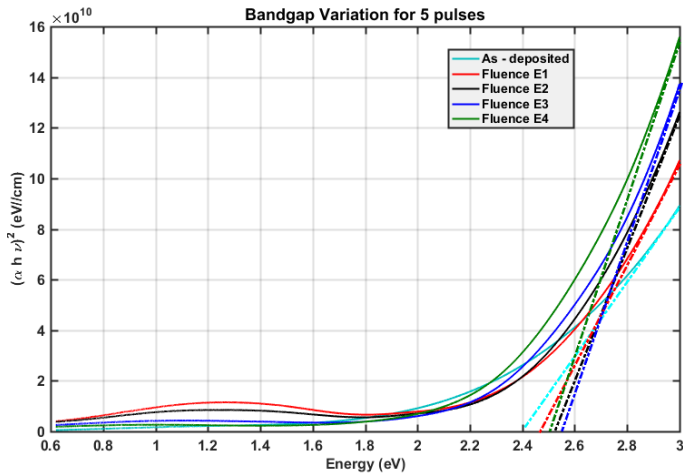


Figure 8: Tauc plot for direct transition band gap of Cu_xS thin films at different optical fluence as compared to as-deposited films

SUMMARY AND CONCLUSIONS

IPL of Cu_xS nanoparticle thin films is demonstrated and the effect of the IPL process parameters on the crystal structure and the properties of the thin film are studied. It is shown that a sintering time of only 2.3 seconds with an energy density of 7.5 J/cm^2 results in a mixture of covellite (CuS) and digenite ($\text{Cu}_{1.8}\text{S}$) phases with reduction of sheet resistance by nearly 99 %. Further, the near IR transmittance reduces by around 47 % and there is a shift in the peak wavelength for transmittance towards the visible spectrum. Increasing the optical energy density to 15 J/cm^2 results in formation of digenite phase only with increased sheet resistance, increased transmittance in the visible range and increased transmittance in the near infrared region. However, increasing the fluence per pulse also involves increasing the sintering time to about 7 seconds which reduces throughput. These observations provide new information on how the process parameters in IPL can be varied to tailor the optical and electrical properties of Cu_xS thin films while balancing IPL process throughput.

ACKNOWLEDGMENTS

The authors gratefully acknowledge the financial support provided for this work by the National Science Foundation grant number CBET #1449383.

REFERENCES

- [1] Grozdanov, I., and Najdoski, M., 1995, "Optical and Electrical Properties of Copper Sulfide Films of Variable Composition," *J. Solid State Chem.*, **114**(2), pp. 469–475.
- [2] Chen, Y. H., Davoisne, C., Tarascon, J. M., and Guery, C., 2012, "Growth of single-crystal copper sulfide thin

films via electrodeposition in ionic liquid media for lithium ion batteries," *J. Mater. Chem.*, **22**(12), pp. 5295–5299.

- [3] Patel, D. K., Kamyshny, A., Ariando, A., Zhen, H., and Magdassi, S., 2015, "Fabrication of transparent conducting films composed of In^{3+} doped CuS and their application in flexible electroluminescent devices," *J. Mater. Chem. C*, **3**(33), pp. 8700–8705.
- [4] De Carvalho, C. N., Parreira, P., Lavareda, G., Brogueira, P., and Amaral, A., 2013, "P-type Cu_xS thin films: Integration in a thin film transistor structure," *Thin Solid Films*, **543**, pp. 3–6.
- [5] Isac, L., Popovici, I., Enesca, A., and Duta, A., 2010, "Copper sulfide (Cu_xS) thin films as possible p-type absorbers in 3D solar cells," *Energy Procedia*, **2**(1), pp. 71–78.
- [6] Isac, L., Duta, A., Kriza, A., Manolache, S., and Nanu, M., 2007, "Copper sulfides obtained by spray pyrolysis - Possible absorbers in solid-state solar cells," *Thin Solid Films*, **515**(15 SPEC. ISS.), pp. 5755–5758.
- [7] Nair, P., Garcia, V., Fernandez, A., Ruiz, H., and Nair, M., 1991, "Optimization of chemically deposited Cu_xS solar control coatings," *J. Phys. D. Appl. Phys.*, **24**, pp. 441–449.
- [8] Sartale, S. D., and Lokhande, C. D., 2001, "Preparation and characterization of copper sulphide thin films using successive ionic layer adsorption and reaction (SILAR) method," *Mater. Chem. Phys.*, **72**(1), pp. 101–104.
- [9] Vas-Umnuay, P., and Chang, C. -h., 2013, "Growth Kinetics of Copper Sulfide Thin Films by Chemical Bath Deposition," *ECS J. Solid State Sci. Technol.*, **2**(4), pp. 120–129.
- [10] Reijnen, L., Meester, B., Goossens, A., and Schoonman, J., 2003, "Atomic Layer Deposition of Cu_xS for Solar Energy Conversion," *Chem. Vap. Depos.*, **9**(1), pp. 15–20.
- [11] Martinson, A. B. F., Riha, S. C., Thimsen, E., Elam, J. W., and Pellin, M. J., 2013, "Structural, optical, and electronic stability of copper sulfide thin films grown by atomic layer deposition," *Energy Environ. Sci.*, **6**(6), p. 1868.
- [12] Sabah, F. A., Ahmed, N. M., Hassan, Z., and Rasheed, H. S., 2016, "Effect of Annealing on the Electrical Properties of Cu_xS Thin Films," *Procedia Chem.*, **19**, pp. 15–20.
- [13] Nair, M. T. S., Guerrero, L., and Nair, P. K., 1999, "Conversion of chemically deposited CuS thin films to and by annealing," *Semicond. Sci. Technol.*, **13**(10), pp. 1164–1169.
- [14] Nien, Y. T., and Chen, I. G., 2009, "Rapid thermal annealing of chemical bath-deposited Cu_xS films and their characterization," *J. Alloys Compd.*, **471**(1–2), pp. 553–556.
- [15] Sanchez-Romaguera, V., Wünscher, S., Turki, B. M., Abbel, R., Barbosa, S., Tate, D. J., Oyeka, D., Batchelor, J. C., Parker, E.A., Schubert, U. S., and Yeates, S. G.,

- 2015, "Inkjet printed paper based frequency selective surfaces and skin mounted RFID tags: the interrelation between silver nanoparticle ink, paper substrate and low temperature sintering technique," *J. Mater. Chem. C*, **3**(9), pp. 2132–2140.
- [16] Bjorninen, T., Virkki, J., Sydanheimo, L., and Ukkonen, L., 2015, "Manufacturing of antennas for passive UHF RFID tags by direct write dispensing of copper and silver inks on textiles," *Proc. 2015 Int. Conf. Electromagn. Adv. Appl. ICEAA 2015*, pp. 589–592.
- [17] Eun, K., Chon, M.-W., Yoo, T.-H., Song, Y.-W., and Choa, S.-H., 2015, "Electromechanical properties of printed copper ink film using a white flash light annealing process for flexible electronics," *Microelectron. Reliab.*, **55**(5), pp. 838–845.
- [18] Hwang, Y. T., Chung, W. H., Jang, Y. R., and Kim, H. S., 2016, "Intensive Plasmonic Flash Light Sintering of Copper Nanoinks Using a Band-Pass Light Filter for Highly Electrically Conductive Electrodes in Printed Electronics," *ACS Appl. Mater. Interfaces*, **8**(13), pp. 8591–8599.
- [19] Dharmadasa, R., Dharmadasa, I. M., and Druffel, T., 2014, "Intense pulsed light sintering of electrodeposited CdS thin films," *Adv. Eng. Mater.*, **16**(11), pp. 1351–1361.
- [20] Dharmadasa, R., Lavery, B. W., Dharmadasa, I. M., and Druffel, T., 2015, "Processing of CdTe thin films by intense pulsed light in the presence of CdCl₂," *J. Coatings Technol. Res.*, **12**(5), pp. 835–842.
- [21] Dhage, S. R., Kim, H.-S., and Hahn, H. T., 2011, "Cu(In,Ga)Se-2 Thin Film Preparation from a Cu(In,Ga) Metallic Alloy and Se Nanoparticles by an Intense Pulsed Light Technique," *J. Electron. Mater.*, **40**(2), pp. 122–126.
- [22] Williams, B. A., Smeaton, M. A., Holgate, C. S., Francis, L. F., and Aydil, E. S., 2015, "Effect of intense pulsed light annealing on the microstructure of copper zinc tin sulfide nanocrystal coatings," **4**, pp. 1–28.
- [23] Gadave, K. M., and Lokhande, C. D., 1993, "Formation of CuxS films through a chemical bath deposition process," **229**, pp. 1–4.
- [24] Güneri, E., and Kariper, A., 2012, "Optical properties of amorphous CuS thin films deposited chemically at different pH values," *J. Alloys Compd.*, **516**, pp. 20–26.
- [25] Quintana-Ramirez, P. V., Arenas-Arrocena, M. C., Santos-Cruz, J., Vega-González, M., Martínez-Alvarez, O., Castaño-Meneses, V. M., Acosta-Torres, L. S., and de la Fuente-Hernández, J., 2014, "Growth evolution and phase transition from chalcocite to digenite in nanocrystalline copper sulfide: Morphological, optical and electrical properties," *Beilstein J. Nanotechnol.*, **5**(1), pp. 1542–1552.